UDK 669.14.018.8:669.18:620.18
Review article/Pregledni znanstveni članek

ISSN 1580-2949
MTAEC9, 40(4)129(2006)

HOT DUCTILITY OF AUSTENITE STAINLESS STEEL WITH A SOLIDIFICATION STRUCTURE

VROČA PREOBLIKOVALNOST AVSTENITNEGA NERJAVNEGA JEKLA S STRJEVALNO STRUKTURO

Franc Tehovnik[1], Franc Vodopivec[1], Ladislav Kosec[2], Matjaž Godec[1]

[1]Institute of Metals and Technology, Lepi pot 11, 1000 Ljubljana, Slovenia
[2]Faculty of Natural Sciences and Technology, Aškerčeva 7, 1000 Ljubljana, Slovenia

Prejem rokopisa – received: 2006-07-01; sprejem za objavo – accepted for publication: 2006-07-24

A survey of the solidification structure of austenitic stainless steels is presented. The solidification occurs, depending on the content of the main alloying elements, with the primary formation of δ-ferrite or austenite. In the case of primary solidification of δ-ferrite, this phase reacts with the residual melt producing austenite with a peritectic reaction. The hot workability of the as-solidified microstructure is better in the case of primary solidification of δ-ferrite, since, in this case, the accumulation of impurities in the final melt is prevented. Some impurities, slightly soluble or insoluble in the solid phase at solidification, e.g., lead, decrease the hot workability significantly, which is also lowered in the case of the segregation of soluble impurities at the boundary of austenite and δ-ferrite. The integrity of the continuous cast slab can be improved and the cracking by hot rolling can be prevented by an optimal adjustment of the steel chemical composition and the parameters of continuous casting. Laboratory tests of one-pass rolling of wedge-shaped specimens of industrial steels have confirmed the recommendations and the conclusions in the quoted references.

Key words: austenitic stainless steels, continuous casting, solidification structure, intergranular cracks and voids, hot workability, effect of impurities

Podan je pregled literature o strjevalni strukturi avstenitnih nerjavnih jekel. Strjevanje se začne v odvisnosti od vsebnosti glavnih legirnih elementov, s primarno kristalizacijo δ-ferita ali avstenita. V primeru primarnega nastanka δ-ferita nastane pri nadaljevanju strjevanja s peritektično reakcijo med trdno fazo in preostalo talino avstenit. Vroča preoblikovalnost jekla s strjevalno mikrostruturo je boljša pri primarni kristalizaciji δ-ferita, ker ta prepreči koncentracijo nečistoč v jeklu v zadnji meddendritni talini. Nekatere nečistoče, ki so netopne ali malo topne v trdni fazi pri kristalizaciji, npr. svinec, močno zmanjšajo vročo preoblikovalnost jekla s strjevalno strukturo, ki se zmanjša tudi zaradi segregacije topnih nečistoč na meji med avstenitom in δ-feritom. Integriteto kontinuirno litih slabov in obseg razpok pri vročem valjanju je mogoče doseči z uravnoteženjem kemične sestave taline in parametrov kontinuirnega litja. Laboratorijski preizkusi z valjanjem klinastih preizkušancev iz industrijskega jekla s strjevalno strukturo v enem prehodu so potrdili sklepe in priporočila v citiranih referencah.

Ključne besede: avstenitna nerjavna jekla, kontinuirno litje, struktura strjevanja, interkristalne razpoke in mikrolunkerji, vroča preoblikovalnost, vpliv nečistoč

1 INTRODUCTION

The hot ductility of steels with a solidification structure, also referred to as the initial ductility, is generally lower than the ductility of the same steel with the microstructure obtained with recrystallization. The explanation for the difference is in the shape and size of the grains, the presence of solidification voids and of impurities and/or segregations at the grain boundaries. After solidification, the grains are coarser and their boundaries frequently oriented orthogonally to the slab surface and to the metal flow by deformation[1]. This and the presence of impurities and segregations increase the propensity to form hot cracks, which in the absence of recrystallization at the following rolling passes, may grow to unacceptable surface defects. Residual elements, such as copper and tin in steels melted from scrap, rejected from the oxide layer to the metal surface my even produce an eutectic melt, wetting the grain boundaries, lowering their resistance and leading to crack formation by the axial flow of the metal[2,3]. Stainless steels are not subjected to this type of hot cracking, because of the sufficient solubility of copper in austenite and the presence of nickel, which prevents the formation of eutectic compositions even in the case of a relatively high content of tin in the steel. It was shown that the addition of nickel decreases the deleterious effect of tin in structural steels with a solidification structure[3].

Stainless steels are iron alloys with chromium, nickel, molybdenum and minor contents of carbon, nitrogen, titanium and niobium as well as different impurities. The presence of a sufficient content of chromium ensures the resistance of the steel to wet and dry corrosion with the formation of a layer of chromium oxide. For a high content of chromium alone, the cold deformability of steel in greatly diminished, with exception of interstitials free steels. This deformability is greatly increased by the addition of nickel ensuring to the steel an austenite matrix with a much better inherent cold deformability than that of the ferrite matrix in pure chromium steels. Other elements are added to stainless steels to achieve specific properties, e. g., molybdenum,

to increase the corrosion resistance in the presence of chloride ions in the corrosion medium; manganese, to bound sulphur in stable sulphide inclusions; nitrogen, to increase the stability of the austenite matrix; niobium and titanium, to bound the residual carbon in stable carbides and prevent, in this way, the formation of chromium carbide precipitates and make the steel susceptible to intergranular corrosion[4]. Silicon and aluminium improve the oxidation resistance of the steel with the formation on the surface of a layer of combined oxide, less permeable to diffusion than pure chromium oxide.

2 THE Fe-Cr-Ni ALLOY SYSTEM

In the binary Fe-Cr[5,6] system the chromium enlarges the field of stability of the α-phase and decreases the field of stability of the γ-phase. For a content of 12 % Cr in the binary Fe-Cr system, the formation of austenite is prevented and, in this way, also all solid-state phase transformations are prevented. Also, other elements, frequently referred to as alphagene elements, enhance the stability of the α-phase, e. g., molybdenum, titanium, silicon and aluminium. Other elements and impurities, like carbon, manganese, nitrogen and copper enhance the stability of austenite.

The greatest solid-solution strengthening is obtained with elements in interstitial solid solution. The connection between the chemical composition of the steel and its microstructure is given very approximately by the Schaeffler diagram[4]. It was, however, established that the content of δ-ferrite, determined using the Schaeffler diagram, can be erroneous. With a magnetic and microstructural assessment, a content of approximately 10 % δ-ferrite was found for an alloy in which according to the Schaeffler diagram the content of δ-ferrite should be approximately 20 %[7]. It is stated in this reference that in the same casting the content of δ-ferrite was in the range 1.5–22.5 %.

The combined alphagene or gammagene effect of elements can be deduced using the chromium and the nickel equivalent[4]:

$$w(\mathrm{Cr_{ekv.}}) = w(\mathrm{Cr}) + 2w(\mathrm{Si}) + 1.5w(\mathrm{Mo}) + 5w(\mathrm{V}) + 5.5w(\mathrm{Al}) + 1.75w(\mathrm{Nb}) + 1.5w(\mathrm{Ti}) + 0.75w(\mathrm{W}) \quad (1)$$

$$w(\mathrm{Ni_{ekv.}}) = w(\mathrm{Ni}) + w(\mathrm{Co}) + 0.5w(\mathrm{Mn}) + 0.3w(\mathrm{Cu}) + 25w(\mathrm{N}) + 30w(\mathrm{C}) \quad (2)$$

3 AUSTENITIC STAINLESS STEELS

These steels are the most used group of stainless steels. The steels are paramagnetic, have a face-centred cubic lattice and excel with a good combination of hot and cold workability, mechanical properties and corrosion resistance. Nickel ensures the stability of the austenite to room temperature, and this effect can be increased by the addition of some gammagene elements, especially nitrogen and copper, while the corrosion resistance is obtained with the proper combination of alphagene elements, chromium, molybdenum, and elements binding carbon and nitrogen to stable compounds. Usually, these steels are classed in two subgroups:

- standard chrom-nickel and chrom-nickel molybdenum austenitic steels,
- chromium-manganese-nitrogen-austenitic steels with a lowered content of nickel and with nitrogen ensuring the stability of austenite[4].

3.1 Solidification of austenitic stainless steels

In industrial conditions the solidification of austenitic stainless steels is not an equilibrium process and a two-phase microstructure of austenite and δ-ferrites is obtained. In dependence of the chemical composition of the melt, particularly on the ratio of alphagene and gammagene elements, the solidification can start with the crystallisation of δ-ferrite or austenite. **Figures 1 and 2** show the as-cast microstructure for two cast laboratory austenitic stainless steels cast in blocks of section (60 × 60) mm[8]. The ratio $w(\mathrm{Cr_{eq}})/w(\mathrm{Ni_{eq}})$ for the steel in **Figure 1** was 1.26, and the content of δ ferrite was 11 %, while for the steel in **Figure 2** the nickel equivalent was of 1.59 and the content of δ-ferrite was 27 %. In the first case, the distribution of both constituents of the microstructure shows that δ-ferrite did solidify from the last interdendritic melt, while in the second case the solidification started with the formation of δ-ferrite. This phase is enriched in alphagene elements, particularly chromium. By annealing and slow cooling chemical homogenisation occurs and the quantity of non-equilibrium δ-ferrite is diminished. It is clear, by comparing the microstructures in **Figures 1 and 2**, that with the primary solidification in austenite greater segregations

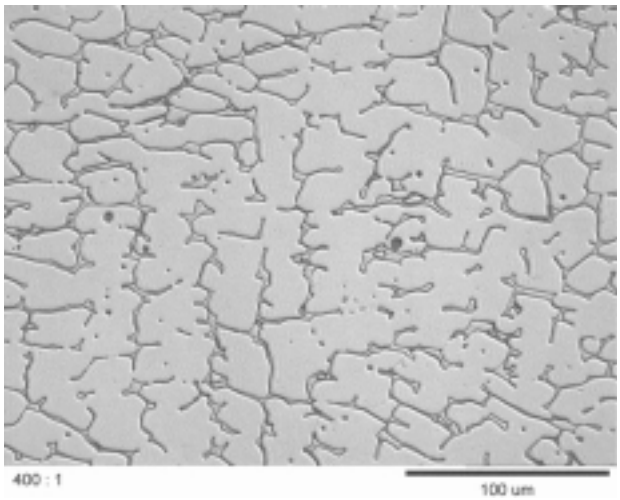

Figure 1: Cast microstructure of austenitic stainless steel with 11 % of δ-ferrite
Slika 1: Lita mikrostruktura avstenitnega nerjavnega jekla z 11 % δ-ferita

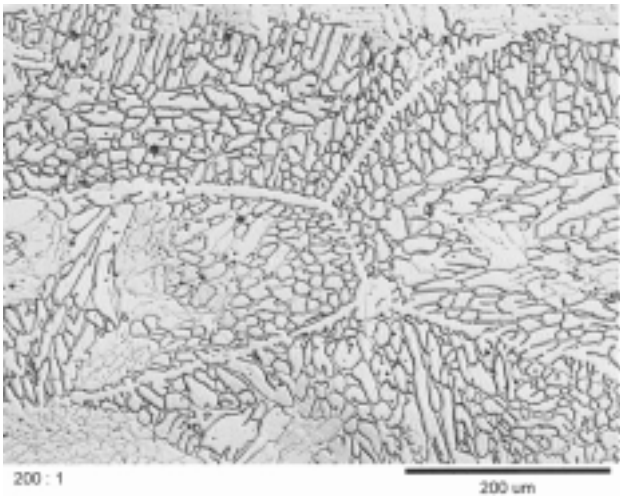

Figure 2: Cast microstructure of austenitic stainless steel with 27 % of δ-ferrite
Slika 2: Lita mikrostruktura avstenitnega nerjavnega jekla z 27 % δ-ferita

are formed and, as a consequence, the hot ductility of the steel with the as-cast microstructure is diminished.

To determine the solidification sequence with accuracy, it is necessary to differentiate between the interdendritic δ-ferrite, as a consequence of the primary solidification in austenite, and the ferrite inside the austenite grains (dendrites), which indicates a primary solidification in ferrite[9,10,11,12]. In the first case, the steel's hot ductility is impaired by the presence of impurities at dendrite boundaries. In the second case, the areas enriched in impurities are situated inside austenite dendrites and their effect on hot ductility is much smaller and, in most cases, not significant. Both solidification sequences are:

$$L = L + \gamma = L + \gamma + \delta = \gamma + \delta \text{ (primary austenite)} \quad (3)$$

$$L = L + \delta = L + \delta + \gamma = \gamma + \delta \text{ (primary δ-ferrite)} \quad (4)$$

3.2 Content and distribution of δ-ferrite in continuous cast steel

The start of solidification with δ-ferrite prevents the formation of areas with lower hot strength in the solidification shell of continuous cast slabs and prevents, in this way, the formation of hot cracks by continuous casting of the stainless steel[13]. The high content of ferrite affects the workability of the steel in the low-temperature range of 600 °C to 900 °C because of its transformation to the brittle σ-phase[14,15]. During continuous casting the cooling rate is relatively high, for this reason, the extent of δ→γ transformation is smaller and more of the δ-ferrite is found in continuous than in conventionally cast steel of the same composition.

The distribution of δ-ferrite in the cross-section of a continuous cast slab depends on the solidification mechanism and the cooling rate[14]. Generally, it was established that the distribution has an approximate form of the letter M, while the local content of δ-ferrite depends on the ratio $w(Cr_{eq.})/w(Ni_{eq.})$[16,17] which basically also affects the solidification sequence of the steel.

In an AISI 304 steel with the equivalent ratio $w(Cr_{eq.})/w(Ni_{eq.}) = 1.83$, the content of δ-ferrite was 4 % near the slab surface, a maximal content of 9 % was found at a distance of 95 mm from the surface, and a lower content in the slab centre. With constant steel chemical composition, the content of δ-ferrite also depends on the solidification rate, although its distribution could be significantly affected by the decomposition by the following cooling regime[18]. With constant steel chemical composition, the higher content of δ-ferrite is found at an intermediate solidification rate.

Investigations on the AISI 304 steel[18] have shown that with primary ferrite solidification austenite is formed along the boundaries of ferrite dendrites with the consumption of the interdendritic melt and of the primary-formed δ-ferrite with a peritectic reaction L + δ = γ. This reaction decreases rapidly the content of the primary δ-ferrite. After the solidification is completed, the decomposition of δ-ferrite to austenite proceeds as a solid-state reaction with the kinetics depending on the diffusion exchange of elements between both phases. For this reason, the content of δ-ferrite depends also on the size of the secondary dendrite arms, which determines the length of the diffusion paths of diffusing elements. The extent of the diffusion exchange of elements between both phases decreases rapidly with the increase of the cooling rate below the peritectic temperature, as this determines the time available for diffusion. The two influencing parameters have opposite effects. The explanation of the M-shaped distribution of δ-ferrite takes in to account also the size of secondary dendrite arms, which increases from the surface towards the centre of the slab, increasing, in this way, the diffusion path necessary for the transformation of the non-equilibrium δ-ferrite to the equilibrium austenite[19,20,21]. Also, the segregation of some elements, which increases for the surface towards the slab centre, affects the content of δ-ferrite. For example, in the AISI 304 steel the segregating elements are nickel, phosphor and manganese, their segregation affects the local value of the ratio of equivalents $w(Cr_{eq})/w(Ni_{eq})$ and the local content of δ-ferrite.

For a value $w(Cr_{eq})/w(Ni_{eq.}) \leq 1.5$ the austenite is the primary solidification phase and the solidification sequence is:

$$L \rightarrow L + \gamma \rightarrow L + \gamma + \delta \rightarrow \gamma + \delta \quad (5)$$

In these conditions, δ-ferrite is found only as a secondary interdendritic phase. In the range $1.48 \leq w(Cr_{eq})/w(Ni_{eq}) \leq 1.95$ δ-ferrite is the primary phase and austenite is also formed with a peritectic reaction and a solid-state transformation.

3.3 Hot cracking during continuous casting and solidification

In the continuously cast slab stresses and deformation are induced by the temperature gradient and the ferrostatic pressure. The capability of the steel to support the deformation without cracking depends on the solidification mechanism, on the steel's high-temperature properties and the presence in the steel of residual elements significantly affecting locally the solidification mechanism and kinetics. Inter-crystalline cracks and voids may appear at the surface and in the interior of the strand because the layer of liquid metal wetting the dendrites' surface breaks with smaller stresses and without plastic deformation. The mechanism of formation of these segregational cracks and voids slightly below the solidification temperature is due to the presence of the elements sulphur, phosphorus, boron, nitrogen and nickel in steel, thus elements who which form intercrystalline segregations and/or low-melting eutectics.

The solidification range of the austenitic and heat-resisting stainless steels is wide and depends strongly on the content of minor elements and impurities. The change from the peritectic to the eutectic solidification process is virtually continuous and gives a solidification structure with primary austenite or δ-ferrite and segregations. The content of δ-ferrite strongly affects the hot workability, and steels with below 2 % are susceptible to hot cracking during the continuous casting. The hot workability is also diminished at a content of δ-ferrite above 6 %[22,23].

The Schaeffler diagram established for the ambient temperature, cannot be used for a discussion on the high-temperature behaviour of the steel. The modified Schaeffler diagram, which can also be used for high temperatures, is an isothermal section of the Fe-Cr-Ni system with, as coordinates, the sum of the alphagene and gammagene elements and the area of susceptibility to hot cracking[24]. Industrial experience shows that steels with primary solidification in δ ferrite are little sensitive to hot cracking.

The susceptibility to hot cracking is increased strongly by primary austenite solidification. The explanation is the large solidification shrinking, the low solubility for sulphur and phosphorus, the small diffusion rate of these elements and the formation of sulphide inclusions from the last melt in the case that the content of steel in manganese is not sufficient for sulphide inclusions to form before the solidification of the last melt. It is possible that sulphur and phosphorus also form grain boundary segregations.

For these reasons, the continuous casting of steels with the ratio $w(Cr_{eq})/w(Ni_{eq}) < 1.5$ is only successful by the optimal combination of several parameters, like a good casting practice, optimization of the steel's chemical composition and the mechanism of solidification, a low content of sulphur and phosphorus, a small melt overheating and the appropriate primary and secondary slab cooling rate.

During the solidification, the melt ahead of the solidification form is enriched in alloy elements, impurities and residuals. The enrichment affects the solidification and with large shrinkage may lead to intercrystalline voids. Cracks do not grow during the solidification, although they can propagate with the following hot working of the slab[24,25,26, 27].

In the solid-liquid range of solidification and with a temperature of approximately 30 % of residual melt, the steel can support only a small load. This temperature is referred to as the "temperature of null strength" (T_{NF}), because the layer of melt cannot transfer the load between the dendrites. With a lower temperature, the solidification of the melt strongly enriched in impurities takes place, and with testing a definite reduction of area is found. This temperature is defined as the "temperature of null hot workability" (T_{NZ}). Below this limit, the reduction of area increases fast to a level depending on the steel composition and it does not change significantly with the further lowering of the temperature, although the steel strength increases continuously.

A secondary decrease of ductility can appear because of the decreased solid solubility of impurities, the formation of precipitates and grain-boundary segregations[28,29,30]. The temperature range between the null strength and the null workability defines the mechanical properties of the steel on the boundary between the liquid and the solid phase. For this reason, the temperature difference $\Delta T_0 = \Delta T_{NZF} = T_{NF} - T_{NZ}$ is a measure of the susceptibility of the steel to form surface cracks and internal voids during continuous casting. Industrial investigations have shown that for a greater temperature difference ΔT_0, a greater extent of hot cracking may occur,[30,31,32] especially with a low ratio $w(Cr_{eq.})/w(Ni_{eq})$. A critical moment is the exit of the strand from the mould, because at this point, the cooling rate and the temperature gradient in the strand are diminished. For this reason, the generation of the solidification heat increases the temperature on the solidification front and may even reach the liquidus temperature. The change of solidification is the explanation for the formation of an area of segregation between the columnar grains near the solidification front. When the slab reaches the first zone of secondary cooling, a sufficient temperature gradient is reestablished[31].

3.4 Effect of sulphur, oxygen and residuals on the hot workability

In stainless steel small amounts of sulphur, phosphorus, oxygen and residuals are also found. The origins of these impurities are: the metal scrap, different non metallic additions, ferroalloys, and the processing itself. Due to the increased use of scrap, the content of

residuals is also continuously increased. Some of the impurities can be eliminated from the melt to a different extent during the processing; however, even a very small content of impurities can affect the hot workability and the formation of surface defects by rolling.

From the binary Fe-Pb system it can be concluded that lead is insoluble in iron[33]. If present in the steel, and due to his low melting temperature, lead wets the surface of the grains or it forms small spherical inclusions in the interior of grains. In the first case, the hot workability of the steel with solidification structure is strongly decreased. For this reason, it is of very great importance, that in all steel processing operations, additions with the lowest possible content of lead are used. The hot workability of the as-cast stainless steel is not decreased at 1200 °C if the content of lead is below 0.0014 %. However, with a lower temperature of 1150 °C the reduction of area is strongly diminished. Even with a content of lead of 10 μg/g and bismuth of 5 μg/g the reduction of area is strongly diminished[34]. A frequently neglected source of lead is the aluminium metal used for de-oxidation of the steel.

In contrast to lead, antimony, tin and arsenic have a limited solubility in solid iron and are, for this reason and their specific physical properties, influential on grain-boundary segregation and may have, with a different the fragilisation mechanism, also a deteriorating effect on the hot workability. For the effect of some elements on hot workability the lead equivalent was proposed [14,35,36]:

$$w(\mathrm{Pb_{eq.}}) = w(\mathrm{Pb}) + 4w(\mathrm{Bi}) + 0{,}025w(\mathrm{Sb}) + 0{,}01w(\mathrm{Sn}) + \\ + 0{,}007w(\mathrm{As}) \quad (5)$$

With the content of all elements in mass fractions *w*/%.

On the basis of results of hot tensile tests it was established that for an acceptable hot workability by primary ferrite solidification a value of $Pb_{eq} < 50$ μg/g is necessary, while for the case of primary austenite solidification the critical value is lower, it is $Pb_{eq} < 30$ μg/g.

Oxygen and sulphur are bound to non-metallic inclusions, whose effect on the hot workability depends on their size, shape and distribution[37]. The effect of sulphide in inclusions can be controlled with the addition of calcium, which changes their shape, size and distribution. Also, with a calcium addition an additional de-oxidation and desulphurization is achieved, since calcium aluminate inclusions of proper composition also bind sulphur, making it possible to achieve an additional purification with rinsing of the steel melt.

4 EXPERIMENTAL WORK

4.1 Hot rolling of wedge-shaped specimens of AISI 316L austenitic steel

The tests were performed in the frame of an industrial investigation aimed at verifying experimentally some suggestions and conclusions quoted in references. The steel chemical composition is shown in **Table 1**. The content of δ-ferrite, determined with magnetic measurements, was relatively high, while, the content of residuals, particularly that of lead, is below the level considered deleterious to the hot workability. The specimens were manufactured from the lower part of a continuous cast slab of thickness 200 mm with one surface and the microstructure as solidified. The content of δ-ferrite in the as-solidified steel was of 9.5 %.

The wedge-shaped specimens were first soaked at a temperature of 1250 °C for 20 min and then the rolling was started at this temperature or at a lower temperature obtained by placing the soaked specimen in a furnace held at a lower temperature. For this reason, the microstructure of the specimens was different only to the extent of a change of the content of δ-ferrite by the 20 min isothermal holding of the specimens cooled from the soaking temperature. The one-pass rolling was carried out in the range of 1250 °C to 950 °C at seven temperatures differing by 50 °C. After rolling, the specimens were quenched or air cooled on a warm bed.

4.2 Microstructure of the steel

The initial content of δ ferrite in the specimen differed to the extent of the transformation δ-ferrite → austenite by the holding of specimens before the rolling test. In **Figure 3** and **Figure 4**, the microstructure of specimens rolled at the temperatures of 1000 °C and 1100 °C is shown for a different extent of one-pass rolling deformation. As shown in these figures, δ-ferrite is found mostly in isolated inserts formed from the last interdendritic melt. Only rarely a thin layer of δ-ferrite was found around some austenite grains. The time interval between the rolling pass and the quenching was 0.5 s to 1 s, too short to allow a significant change of the microstructure formed during the rolling pass. Also, virtually no difference was found in the share of recrystallization between air-cooled and quenched specimens. It is concluded that the recrystallization occurred only during, and immediately after, the rolling pass. For this reason, the microstructure will be referred to as the rolling microstructure. The distribution of δ-ferrite in the specimens rolled at low temperature and

Table 1: Chemical composition of the investigated steel in mass fractions *w*/%
Tabela 1: Kemična sestava jekla v masnih deležih *w*/%

Steel	C	Si	Mn	P	S	Cr	Ni	Mo	Cu	Al	N	Pb	Sn
316L	0.02	0.34	1.55	0.033	0.002	17.6	10.2	2.07	0.33	0.005	0.025	0.0016	0.005

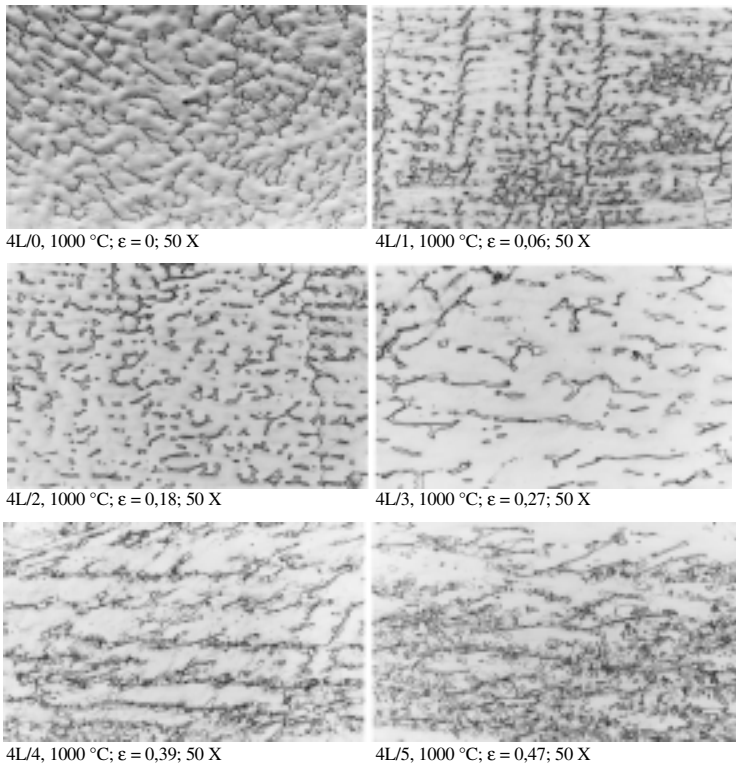

4L/0, 1000 °C; ε = 0; 50 X
4L/1, 1000 °C; ε = 0,06; 50 X
4L/2, 1000 °C; ε = 0,18; 50 X
4L/3, 1000 °C; ε = 0,27; 50 X
4L/4, 1000 °C; ε = 0,39; 50 X
4L/5, 1000 °C; ε = 0,47; 50 X

Figure 3: Microstructure of the steel deformed with one-pass rolling at 1000 °C for a different extent of deformation. Electrolytic etching in a solution of 10 % $C_2H_2O_2*2H_2O$, air cooling

Slika 3: Mikrostruktura deformiranega jekla pri temperaturi valjanja 1000 °C z enim vtikom v odvisnosti od stopnje deformacije. Elektrolitsko jedkano v 10-odstotni raztopini $C_2H_2O_2*2H_2O$, ohlajeno na zraku

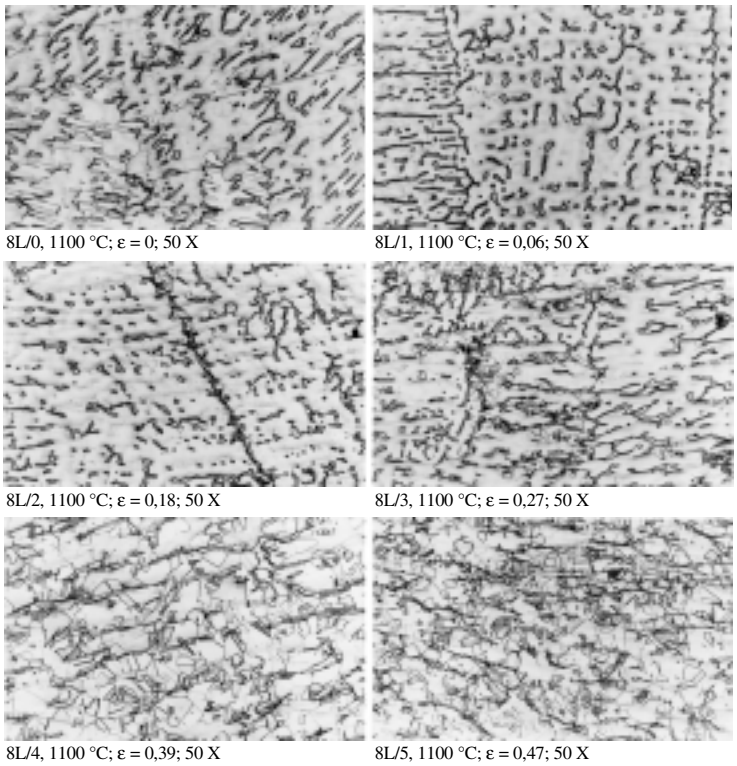

8L/0, 1100 °C; ε = 0; 50 X
8L/1, 1100 °C; ε = 0,06; 50 X
8L/2, 1100 °C; ε = 0,18; 50 X
8L/3, 1100 °C; ε = 0,27; 50 X
8L/4, 1100 °C; ε = 0,39; 50 X
8L/5, 1100 °C; ε = 0,47; 50 X

Figure 4: Microstructure of the steel deformed with one-pass rolling at 1100 °C for a different extent of deformation. Electrolytic etching in a solution of 10 % $C_2H_2O_2*2H_2O$, air cooling

Slika 4: Mikrostruktura deformiranega jekla pri temperaturi valjanja 1100 °C z enim vtikom v odvisnosti od stopnje deformacije. Elektrolitsko jedkano v 10-odstotni raztopini $C_2H_2O_2*2H_2O$, ohlajeno na zraku

low deformation was similar to that after soaking, while at higher temperature it was changed to the extent of the deformation and of the recrystallization.

At the rolling temperature of 1000 °C the first recrystallized grains were observed after 40 % of deformation, while a similar recrystallization was observed at the lower temperature of 950 °C only with a deformation over 50 %. With a temperature above 1000 °C the extent of recrystallization increased very rapidly and, e. g., after the rolling at 1100 °C the first recrystallization nuclei were found with a deformation of approximately 25 %, while with a deformation of 40 % most of the microstructure was recrystallized. The recrystallization nuclei were in all cases observed to

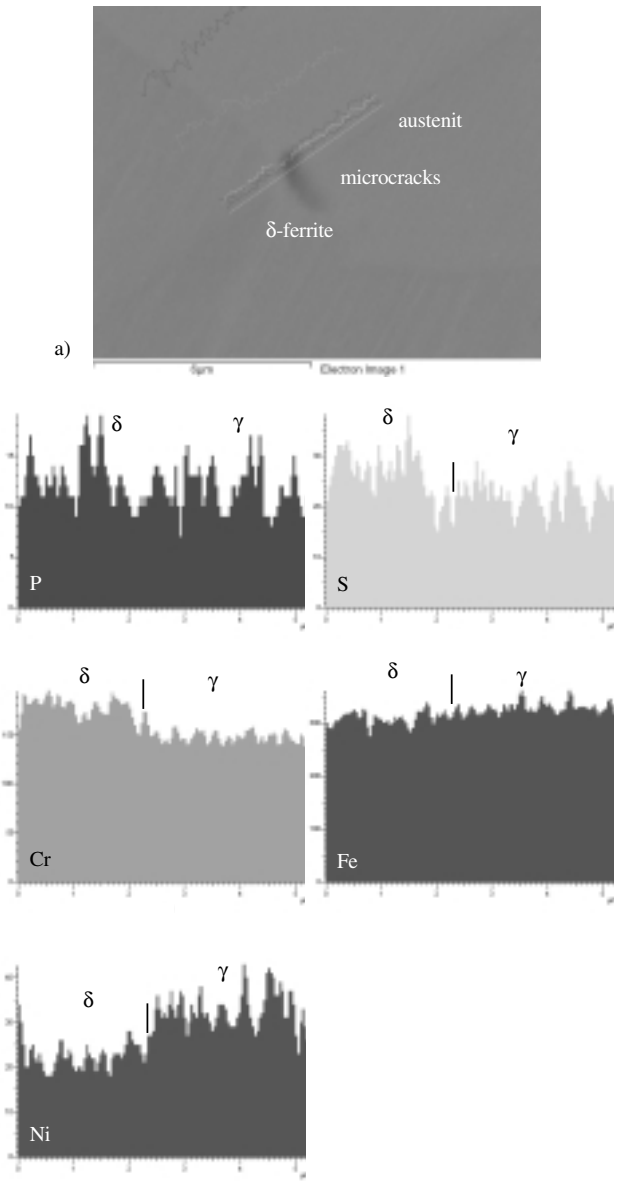

Figure 5: Distribution of different elements by line scanning from δ-ferrite to austenite

Slika 5: Porazdelitev različnih elementov z EDS-analizo preko polja δ-ferita in avstenita

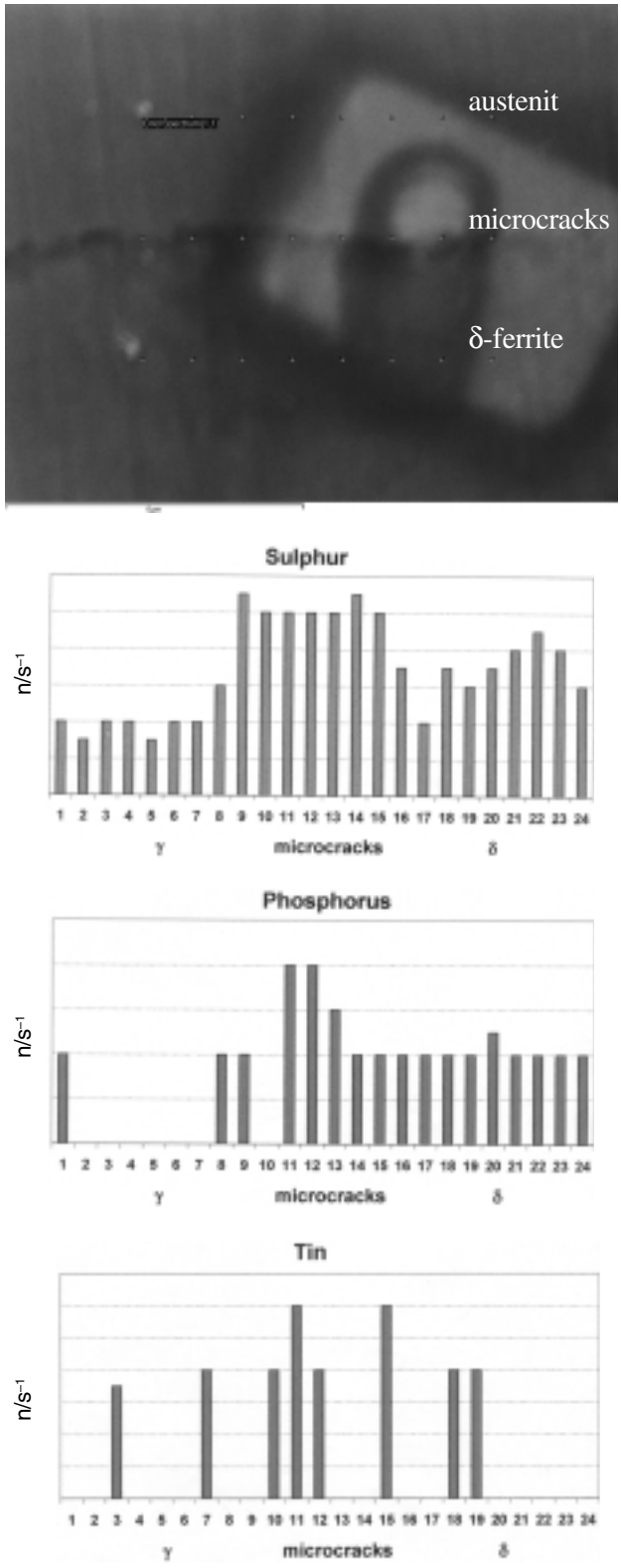

Figure 6: Point analysis on the boundary between δ-ferrite and austenite. The content of elements is given in cps (counts per second), which is proportional to the local content of the analysed element

Slika 6: Točkovna analiza na meji δ-ferita in avstenita. Vsebnost elementov je dana v s^{-1} (številu impulzov na sekundo), ki je proporcionalna lokalni vsebnosti elementa

form at austenite grain boundaries, δ-ferrite-austenite boundaries, twin boundaries and non-metallic inclusions, and never inside the δ-ferrite areas. Thus, the presence of δ-ferrite enhances the nucleation of recrystallized grains and increases, in this way, the recrystallization rate.

After rolling at 1100 °C and 1150 °C and with great deformation, cracks were found on the surface and particularly on the edges of the specimens. The chemical analysis on the surface of the opened cracks showed only chromium and iron oxides. In the inside of specimens some microcracks were found, particularly on the boundaries between austenite and δ ferrite. In **Figure 5 a** line scan is shown from δ-ferrite over the phase boundary to austenite. As expected, the content of chromium and molybdenum is higher in δ-ferrite, the content of nickel is higher in austenite, while the content of iron is virtually equal in both phases. It is evident that the kinetics of the solution of δ ferrite depends on the diffusion exchange of chromium and nickel atoms between both phases. The decomposition of δ-ferrite is, thus, temperature and time dependent. The chemical sensitivity of the analysis was too small to show a difference in the content of sulphur and phosphorus in both phases. Also, with the line scan over the boundary between both phases it was not possible to identify an eventual grain-boundary segregation. However, with point counts it was possible to show a difference in the intensity of the signal of Kα radiation for the content of sulphur in the boundary and the ferrite and the austenite phases. Similar results were found by point analysis also for phosphorus and tin (**Figure 6**). These findings confirm that the concentration of impurities is increased at the grain boundary.

These findings are in agreement with industrial data showing a more frequent surface cracking for steels with a higher content of δ-ferrite.

With other parameters constant, the content of δ-ferrite depends on the soaking temperature and on the temperature (**Figure 7**). After greater deformation, the content of the δ-ferrite was found to be lower; however, this may be due to the inaccuracy of the measurements, since, after greater plastic deformation, the thickness of ferrite domains is small and the measuring method may be less reliable.

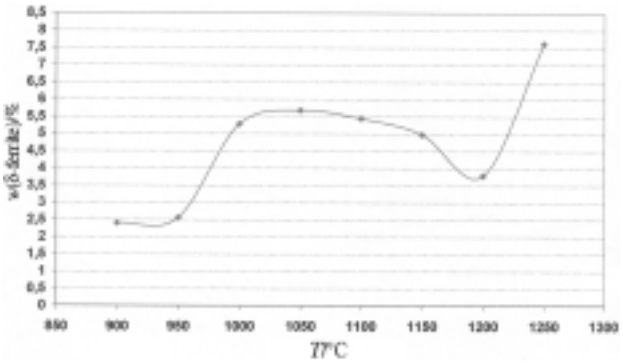

Figure 7: Dependence of the content of δ ferrite on the temperature after cooling from 1250 °C. Soaking time 20 min.

Slika 7: Vsebnosti δ-ferita v odvisnosti od temperature žarjenja po ohladitvi s 1250 °C. Trajanje žarjenja 20 min.

5 CONCLUSIONS

- The hot ductility of continuously cast austenitic stainless steels depends strongly on the solidification mechanism, and better hot ductility is obtained when δ ferrite is the primary solidified phase.
- The hot ductility also depends on solidification defects, such as intercrystalline voids and cracks formed in the region of low strength of the solidified layer at the slab surface, the content of some residual elements with low solid solubility in austenite and elements with a tendency to form segregations on the boundary between the austenite and the δ-ferrite.
- An acceptable ductility and integrity of the surface of the continuously cast slab is obtained with a proper adjustment of the chemical composition of the steel, with special consideration of the content of different impurities, to the slab casting temperature and cooling rate.
- Cracks form most frequently in the area of the exit of the slab from the mould, where the cooling and solidification rates are significantly decreased.
- For a given chemical composition and continuous casting procedure, the content of δ ferrite depends strongly on the soaking temperature.
- Industrial steel with a solidification structure with up to 12.5 % of δ-ferrite supports the one-pass rolling deformation of up to 60 % without surface cracking. Only at rolling temperatures of 1100 °C and 1150 °C occasional edge cracks were observed with a very high per-pass rolling deformation.

6 REFERENCES

[1] F. Vodopivec, M. Torkar, M. Debelek, F. Haller, F. Kaučič: Mat. Sci. Techn. 4 (**1988**), 917

[2] D. A. Melford: JISI 204 (**1966**), 49

[3] M. Torkar, F. Vodopivec: Železarski zbornik 15 (**1981**), 61

[4] Stainless Steels: ASM International, 1994

[5] Honeycombe R., Hancook P.: Stels microstructure and properties, 2nd edition, University of Cambridge, 1995

[6] Rivlin V. G., Raynor G. V.: Int. Met. Rev., 25 (**1980**), 21

[7] C. Jannson: Degradation of cast stainless steel elbows after 15 years of service; Fontenvraud Inter. Symp., 10–14 sept. 1990, Royal Abbey of Fontevraud, France, Loc cit.: H. M. Chung, T. R. Leax: Mater. Sci. Techn. 6 (**1990**), 249

[8] J. Vojvodič-Tuma, D. Kmetič, B. Arzenšek, F. Vodopivec, B. Šuštaršič, B. Breskvar: submitted to publication in NED

[9] A guide to solidification of steels, Jernkontoret, Stockholm, Sweden, (**1977**), 81–132

[10] J. A. Brooks, A. W. Thompson: Int. Mater. Rev., 36 (**1991**), 16

[11] Shigeo Fukumoto, Wilfried Kurz: Solidification phase and microstructure selection maps for Fe-Cr-Ni alloys, ISIJ International, 39 (**1999**) 12, 1270–1279

[12] Shigeo Fukumoto, Wilfried Kurz: Prediction of the d to g transition in austenitic stainless steels during laser treatment, ISIJ International, 38 (**1998**) 1, 71–77

[13] G. Jolley, J. E. Geraghty: Solidification and casting of metals, London, The Metals Society, 1979, 411–415

[14] L. Myllykoski, N. Suutala: Efect solidification mode on hot ductility of austenitic stainless steels, Metals Technology, December, 10 (**1983**), 453–460

[15] B. Weiss, R. Stickler: Phase instabilities during high temperature exposure of 316 austenitic stainless steel, Metallurgical Transactions, 3 (**1972**), 851–865

[16] M. Wolf: Ironmaking Steelmaking, (**1986**) 13, 248–257

[17] J. E. Lait, J. K. Brimacombe, F. Weinberg: Ironmaking Steelmaking, 1 (**1974**), 90–97

[18] S. K. Kim, Y. K. Shin, N. J. Kim: Distribution of d-ferrite content in continuously cast type 304 stainless steel, Ironmaking and Steelmaking, 22 (**1995**) 4, 316–325

[19] O. J. Pereira, J. Beech: Solidification technology in the foundry and casthouse, London, The Metals Society, 1983, 315–321

[20] N. Suutala, T. Takalo, T. Moisio: Metall. Trans., 10A (**1979**) 8, 1183–1190

[21] N. Suutala, T. Takalo, T. Moisio: Metall. Trans., 11A (**1980**) 5, 717–725

[22] F. Tehovnik, B. Arh, D. Kmetič, B. Arzenšek, M. Klinar, A. Kosmač: Optimizacija pogojev litja na kontinuirni napravi in vroči valjarni pri izdelavi jekel Acroni 19 in Acroni 19Si, Research report of the Institute of metals and technology (in Slovene), Ljubljana, 2002

[23] Suutala N.: Dr.-thesis, University of Oulu, 1982

[24] P. R. Scheller, W. Bleck, R. Flesch: Efect of residual elements on hot-crack susceptibility of austenitic stainless steel, Steel Research int. 75 (**2004**) 10, 672–679

[25] K. D. Unger, W. Biesterfeld, F. Berentzen, R. Thielmann: Metallurgical problems encountered in stainless steel continuous casting, Paper 61

[26] Bishop H. F., Ackerlind C. G., Pelini W. S.: Transations American Foundrymens Society, 60n (**1952**), 818–833

[27] H. G. Baumann, E. A. Elsner, J. Pirzun: Stahl und Eisen, 191 (**1971**), 39–147

[28] Schmidtmann E., Merz M.: Steel Research, 58 (**1987**) 4, 191–196

[29] Schmidtmann E., Ebrecht M.: Steel Research, 62 (**1991**) 11, 522–527

[30] Schmidtmann E., Rakoski F.: Archiv Eisenhuttenwesen, 54 (**1983**), 357–368

[31] Schmidtmann E., Pleugel L.: Archiv Eisenhuttenwesen, 51 (**1980**), 49–58

[32] Scheller P. R., Flesch R.: Hochtemperatureigenschaften der Strangschale (Erhohung des Anteils stranggiessbarer Stahlsorten), EUR Report 13240/1 DE (1991)

[33] Hansen M.: Construction of binary alloys, 1965

[34] Ljungstrom L. G.: The influence of trace elements on the hot ductility of austenitic 17 Cr 13 Ni Mo-steel, Scandinavian Journal of Metallurgy 6 (**1977**), 176–184

[35] Norstrom L. A.: Scandinavian Journal of Metallurgy 8 (**1979**), 95–96

[36] L.G. Ljungstrom: Scandinavian Journal of Metallurgy 11 (**1982**), 139–142

[37] Sellars C. M. and Tegart W. J. Mcg.: Int. Metall. Rev., 17 (**1972**), 1–24